scientific reports

Check for updates

OPEN

A synchrotron-based kilowatt-level radiation source for EUV lithography

Bocheng Jiang[1,2], Chao Feng[1,2]✉, Changliang Li[1], Zhenghe Bai[3], Weishi Wan[4], Dao Xiang[5], Qiang Gu[1,2], Kun Wang[1,2,6], Qinglei Zhang[1], Dazhang Huang[1,2] & Senyu Chen[7]

A compact damping ring with a limited circumference of about 160 m is proposed for producing kilowatt-level coherent EUV radiation. The electron bunch in the storage ring is modulated by a 257 nm wavelength seed laser with the help of the angular-dispersion-induced micro-bunching method (Feng and Zhao in Sci Rep 7:4724, 2017), coherent radiation at 13.5 nm with an average power of about 2.5 kW can be achieved with the state-of-the-art accelerator and laser technologies.

Radiation from accelerator-based light sources for optical lithography had been studied for a long time[1,2]. Accelerator-based light sources for lithography get several advantages. They are clean light sources without debris contaminating the optics and they are convenient to tune the wavelength without a major technical change. It has been confirmed by the semiconductor industry that 13.5 nm wavelength extreme ultraviolet (EUV) lithography will be the route for the advanced wafer manufacturing. High power EUV light source is one of the key technologies for EUV lithography. The EUV source of average power beyond 500 W is the cutting edge of the research both for laser-produced plasma (LPP) light sources and accelerator-based light sources.

Yet, the average power of the spontaneous EUV radiation from an electron storage ring is only several watts even with extremely high beam current and long undulators. Using micro-bunched electron beams is currently the most effective way to enhance the average power of accelerator-based light sources, since the output power is proportional to the square of the electron numbers in the micro-bunches[3,4]. For storage rings, the leading concept for realizing this kind of light source is the steady-state micro-bunching (SSMB)[5–7] scheme. One of the critical issues of SSMB is how to further compress the micro-bunch to make it shorter than the EUV wavelength on a turn-by-turn basis.

Micro-bunches with durations at the EUV and soft X-ray wavelength scale can be achieved by utilizing the angular-dispersion-induced micro-bunching (ADM) technique[8], which can precisely tailor the electron beam longitudinal distribution with the aid of an optical laser. With proper setting of the modulation amplitude and the dispersion chicane, the bunching factor at nth harmonic can be written as:

$$b_n = J_n\left(nk_s\xi\frac{\Delta\gamma}{\gamma}\right)e^{-\frac{1}{2}\left(nk_s\eta\sigma_{y'}\right)^2}, \tag{1}$$

where k_s is the wave number of the seed laser, ξ, η are the momentum compaction and dispersion function of the dispersive chicane respectively, γ is the relativistic parameter for the beam energy, $\Delta\gamma$ is the energy modulation amplitude induced by the seed laser. $\sigma_{y'}$ is the vertical angular divergence of the electron beam. When $\sigma_{y'}$ is extraordinary small, unprecedented high harmonic radiation can be achieved.

However, this manipulation process, or so-called the modulation, will increase the electron beam energy spread and the vertical emittance, resulting a limited repetition rate[9] even with a demodulation[10] that cancels most parts of them. For the EUV radiation purpose, the beam energy is optimized to a few hundreds of MeV. For such a low energy storage ring, the synchrotron radiation damping is very weak, the damping time is several tens or even hundreds of milliseconds. The residual perturbation caused by the modulation needs thousands of turns

[1]Shanghai Advanced Research Institute, Chinese Academy of Sciences, Shanghai 201204, China. [2]Shanghai Institute of Applied Physics, Chinese Academy of Sciences, Shanghai 201800, China. [3]National Synchrotron Radiation Laboratory, USTC, Hefei 230029, China. [4]School of Physical Science and Technology, ShanghaiTech University, Shanghai 201210, China. [5]Key Laboratory for Laser Plasmas (Ministry of Education), School of Physics and Astronomy, Shanghai Jiao Tong University, Shanghai 200240, China. [6]University of the Chinese Academy of Sciences, Beijing 100049, China. [7]Institute of High Energy Physics, Chinese Academy of Sciences, Beijing 100049, China. ✉email: fengchao@zjlab.org.cn

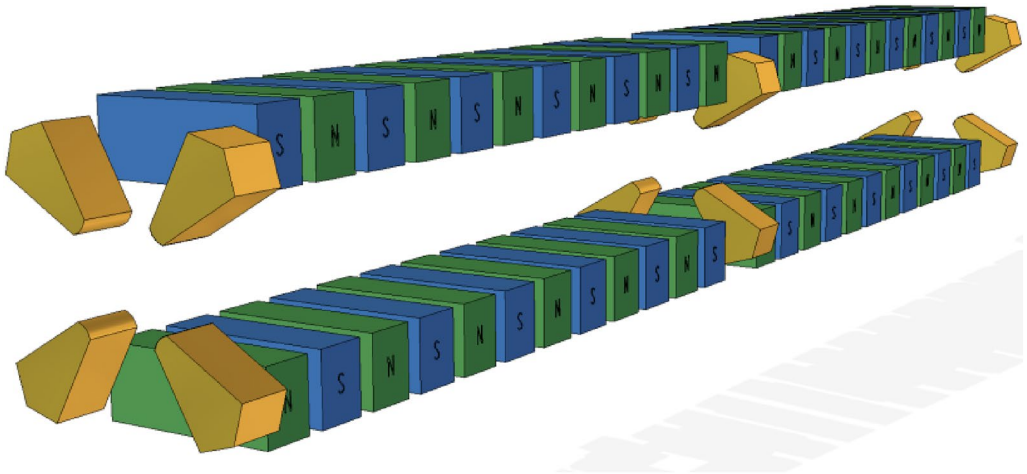

Figure 1. Schematic view of equally focused wiggler.

being damped down. A storage ring with shorter damping time is highly desired to eliminate the perturbations rapidly and to achieve a higher modulation repetition rate as well as getting higher average radiation power.

Damping rings have been widely investigated for colliders[11–13]. Damping wiggler is an indispensable device in the damping ring that reduces both the damping time and transverse emittances. Nevertheless, the vertical focusing effect of the strong damping wiggler will significantly distort the linear beam optics, especially when the beam magnetic rigidity (beam energy) is low (hundreds of MeV), sometimes the periodic lattice solutions do not exist anymore[14]. In medium energy rings, superconducting wigglers (SWs) with limited length are used for both colliders and synchrotron radiation facilities[15–17]. Long SWs in the medium energy storage ring will create huge radiation power, makes great technical challenges for photon absorbers[18]. More seriously, the damping wiggler also contributes remarkable nonlinear effects that may shrink the dynamic aperture (DA) and the momentum aperture (MA)[19], resulting in a limited lifetime of the electron beam.

In this paper, a compact EUV light source that combines the damping ring and the ADM techniques is proposed. A storage ring equipped with SWs is adopted to significantly shorten the dumping time, supporting the generation of high repetition EUV radiation with the ADM technique in a bypass line. The beam is kicked into the bypass beam line for radiation and then re-injected into the storage ring (for reusing) at a much lower repetition rate than the beam evolution frequency in the storage ring. A special design for SWs with quadrupole poles inside is given and studied. The MA of the damping ring is optimized to a large value and a dedicated demodulation lattice in the bypass line is given to ensure a reasonable beam lifetime for high current operation. Three-dimensional simulations have been performed and the results indicate the generation of kilowatt-level EUV radiation at 13.5 nm with current available technologies.

Equally focused wiggler

The wiggler magnet with wide enough poles presents a longitudinal field written as[14],

$$B_z = B_0 \sin(k_p z)\sinh(k_p y) = B_0 \sin(k_p z)\left(k_p y + \frac{(k_p y)^3}{3!} + \ldots\right), \tag{2}$$

where z is the longitudinal direction along beam axis. When the beam wiggles in the horizontal plane, B_z will produce a vertical force. In Eq. (2), B_z is proportional to y for the first order approximation which acts as a quadrupole field in vertical (V) plane. While in horizontal (H) plane, the beam acts likely passing through a drift. The transfer map difference between V/H planes makes it difficult to match in the ring.

This difference can be eliminated by designing the wiggler poles as wedge magnets[14]. This method is effective when magnetic field is not so strong. For the strong wigglers such as SWs, the limited wedge angle is insufficient to balance the focus between V/H planes. Several types of planar wigglers, such as the alternate pole canting wiggler, had been proposed to produce additional horizontal focusing[20,21]. However, these field manipulation methods are convenient for the permanent magnet wiggler. While for SWs, the magnet field is beyond saturation of the yoke, the quadrupole field quality is difficult to control by introducing gradient of the poles.

Here we propose inserting sets of quadrupoles in the wiggler to balance the transverse focuses in both planes. The schematic layout of the design is given in Fig. 1, where the poles of orange color are quadrupoles. The equally focused wiggler is composed by a segment of wiggler followed by a quadrupole and in repetition. This model is simulated by ELEGANT code[22] with canonical integration method. The structure is compact and effective, identical transfer matrices can be found in both planes with proper choice of the parameters as shown in Table 1.

The optimized beta functions are shown in Fig. 2, where the beta functions are low and in periodicity. In this setting, the technical challenges had been fully considered, the wiggler is segmented to 3 sections, each section holds two segments 0.9 m wiggler sandwiched by two 0.1 m and one 0.2 m long quadrupoles. Two 0.4 m drift

Parameters	Value
Beam energy (MeV)	1000
Period length (mm)	60
Periods per segment	15
Peak magnetic field (T)	5.66
Quad Gradient family 1 (T/m)	13.1
Quad Gradient family 2 (T/m)	10.3
Pole gap (mm)	10

Table 1. Beam parameters for equally focused superconducting wiggler.

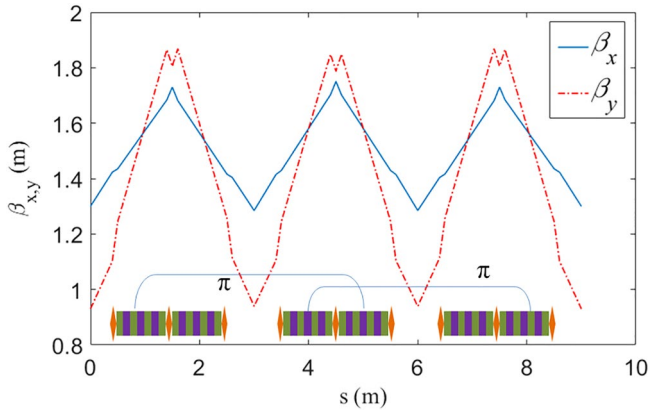

Figure 2. Beta functions in the wiggler.

space at both ends for cryogenic tank had been reserved, making sure a reasonable length of 3.0 m for each wiggler. The peak magnetic field of the wiggler is 5.66 Tesla which is achievable with superconducting techniques.

Since the betatron phase advances of the wiggler in H/V planes are both 2π, there are many π nodes as shown in Fig. 2, which cancels most parts of the nonlinear kicks and shapes a good nonlinear performance, as will be shown in the following section.

Unlike the Robinson wiggler[23,24], for this study the wiggler is place at the dispersion free straight section. The quadrupole fields combining with the wiggler field will not redistribute the damping partition number.

It is worth to stress here that the helical undulator can also produce both horizontal and vertical focus naturally. However, by increasing the field of the helical undulator, it will excite the vertical emittance which is not compatible with the ADM scheme as a tiny vertical emittance is highly required. This is the reason that helical undulator is not adopted in our design.

Damping ring with large momentum acceptance

For high power EUV radiation from a micro-bunched electron beam, we need beam in a storage ring with peak current more than 100 A, this may result severe intra beam scattering (IBS) and Touschek effects. A relative high beam energy of 1 GeV is chosen to mitigate those effects yet the energy is still suitable for EUV radiation. The Touschek lifetime strongly depends on the MA. For a low energy and high peak current ring, local momentum aperture (LMA) is the majorly consideration of the lattice design which is bounded by the nonlinear beam dynamics. LMA is usually lower in the arc where the dispersion is nonzero. The LMA will be reduced when the dispersion is increased. The way to reduce the dispersion without rapidly raising the sextupole strength is to increase the number of the lattice cells. While considering the ring needs to be as compact as possible to get cost competitive, the number of cells is eventually chosen to be 8. There are 8 straight sections, 6 of them are accommodated by SWs, the other 2 are for injection, extraction and RF system.

Triple-bend achromat (TBA) lattice was designed for the ring. To have a compact configuration, all bending magnets are combined-function ones. There are 3 families of chromatic sextupoles in the lattice. The two defocusing sextupoles of the same family close to the matching bending magnets have the highest integrated strength, and the horizontal betatron phase advance between these two sextupoles is about π, which is beneficial for enlarging horizontal dynamic aperture. The fractional parts of the horizontal and vertical tunes of each lattice cell are near (3/8, 5/8) for nonlinear dynamics cancellation over 8 cells.

The beam parameters with/without considering IBS effects are shown in Table 2. The beta and dispersion functions of a half ring are shown in Fig. 3 and the LMA of a half ring gotten through tracking is shown in Fig. 4.

The LMA is tracked using Elegant, it is clear that LMA is smaller in the arc where dispersion is large. The IBS effect is evaluated also using Elegant based on Bjorken–Mtingwa's formula taking account all Twiss parameters

	W/O IBS	W/O IBS	With IBS
	W/O SW	With SW	
Beam energy (MeV)	1000	1000	1000 MeV
Circumference (m)	80	158.4	158.4
Tune (x/y)	11.25/5.15	18.27/12.17	18.27/12.17
Horizontal emittance (nm·rad)	3.07	0.42	1.35
Energy spread	6.63e-4	1.01e-3	1.18e-3
Energy loss per turn (MeV)	0.046	0.704	0.704
Damping time (x/y/s) (ms)	7.7/11.5/7.7	1.45/1.49/0.76	1.45/1.49/0.76
RF frequency (MHz)	–	–	499.65
RF voltage (MV)	–	–	1.2
Harmonic number	–	–	264
Bunch charge (nC)	–	–	8.28
Bunches	–	–	190
Bunch length (mm)			9.0
Beam current (A)	–	–	3.0
Peak current (A)	–	–	111
Betatron coupling	–	–	0.7%
Touschek lifetime (h)	–	–	0.5

Table 2. Ring parameters.

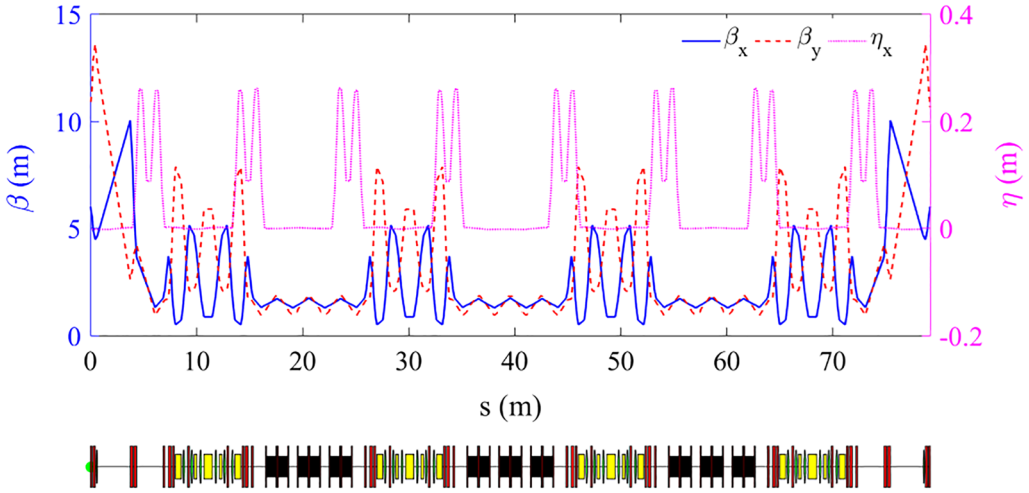

Figure 3. Beta and dispersion functions of a half ring.

along the ring to calculate beam size. The horizontal emittance is more than tripled when counting IBS effect as the peak current reaches 111 A. This prevent us seeking a higher peak current because a larger horizontal emittance will worse de-modulation result thorough T_{511}, T_{522}, T_{521} terms as will be explained later.

The nonlinear effects of SWs are under well control, owing to π nodes in the wiggler which cancels most of parts the nonlinear kicks. The beta function in the wiggler is small, which minimizes the nonlinear effects. As shown in Fig. 4, the LMA in the arc is more than 2.5%.The DA of the ring, as shown in Fig. 5, is about 10 mm in horizontal plane. The main optimization target of this ring is a relatively large LMA which is of great importance for the Touschek lifetime, DA has not been fully optimized, but is large enough for injection. The biggest challenge of nonlinear beam dynamics in this case is not SWs, but matching two long straight sections reserved for the RF cavity and injection/extraction elements. Long straight sections break the symmetry of the ring, arousing high-order driving terms that deteriorate nonlinear performance.

High power EUV generation

Based on the above storage ring, ADM scheme is utilized to generate micro-bunches and enhance the EUV radiation. In order to get a large bunching factor, we need the injection beam with small angular divergence, which means a large vertical beta function and zero alpha function[9] at the point of the vertical bend B_0. After the electron beam passes through the vertical bend B_0, the electron beam with different initial energy spread will have

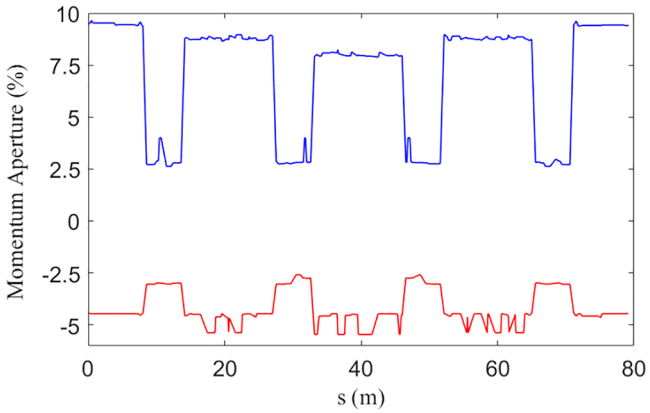

Figure 4. Local momentum aperture of a half ring (blue/red curve is the positive/negative momentum limit respectively).

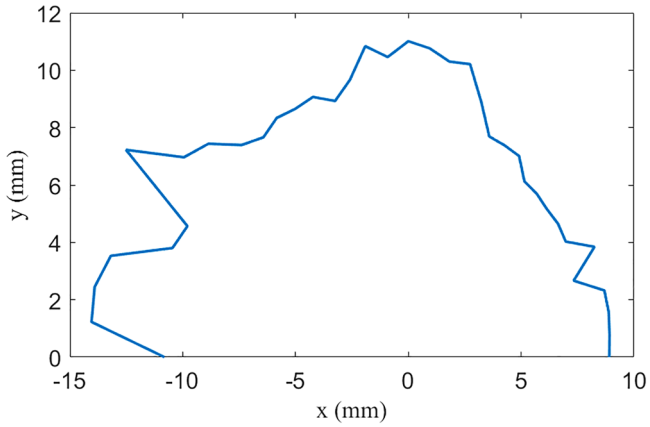

Figure 5. Dynamic aperture with superconducting wiggler.

Bending angle of B_0 (mrad)	9.5
Length of B_0 (m)	0.3
Laser wave length (nm)	257
Energy modulation amplitude (σ_{E0})	0.6
R56 of dogleg	−6.15e−5
Dispersion of dogleg (mm)	6.5
Distance between two bends in dogleg (m)	0.265

Table 3. Parameters for ADM.

different angular dispersion. Then the electron beam interacts with an external laser with central wavelength of 257 nm in the modulator (M). After the energy modulation, the electron beam goes through a dispersion section called dogleg, which can convert the energy modulation into the density modulation. Micro-bunches can be realized by properly setting the bending angle of B_0, the energy modulation amplitude and the dispersion of the dogleg. The main parameters for ADM are given in Table 3. The micro-bunched beam can emit temporal coherent radiation through the radiator (R).

When the electron beam interacts with the laser in the modulator the energy spread will be inevitably increased. The vertical dispersion in the modulator is nonzero, which causes a vertical emittance growth simultaneously. To achieve high average power, we need to improve the repetition rate of the coherent radiation, thus the demodulation (D-M) of the electron beam is necessary to erase the energy modulation as to perturb the electron beam as less as possible. For this purpose, the seed laser has been split into two branches with a phase shift of π and interact with the same electron beam in the M and D-M to cancel the energy modulation.

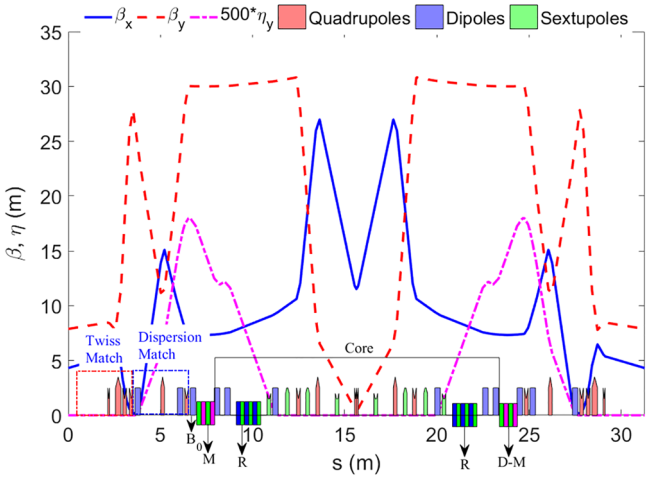

Figure 6. Beam optics for bypass section.

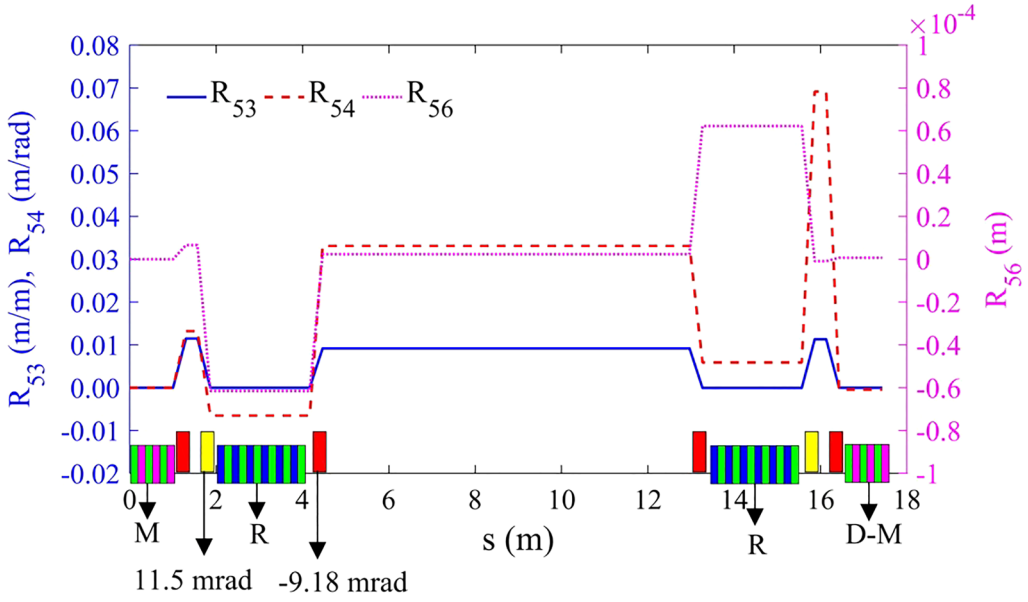

Figure 7. The transfer matrix terms R_{53}, R_{54} and R_{56} along the *core* section. The bottom of the figure contains the layout of the vertical bends. The red rectangle represents the reverse vertical bend, and the yellow rectangle represents normal vertical bend.

Figure 6 shows the lattice design for M and D-M beam line. The beam line gets five quadrupoles in the center with two vertical bends at both sides forms a double bend achromatic (DBA)-like structure. The R_{56} generated by the doglegs is cancelled by the DBA structure, so that the R_{56} between M and D-M is zero, under which condition the demodulation is the most effective. Figure 7 shows the transfer matrix terms R_{53}, R_{54} and R_{56} along the core region. For clear observation, only the longitudinal positions of the vertical bend, modulator and radiator are shown in the figure. In fact, in order to maximize the effect of the demodulation, the beam line between M and D-M are not only required to be isochronous, but also the transfer matrix terms related to the longitudinal displacement, such as the first-order terms R_{53}, R_{54} and the second-order terms T_{511}, T_{521}, T_{533}, T_{566}, should be as small as possible (there is no horizontal bend, so R_{51}, R_{52} are all zero naturally). This ensures that the phase space of the electron beam at the M and the D-M is the same, so after demodulation, the electron beam can return to its original state.

The beam line is symmetric, which has many advantages. It ensures that the transport line is achromatic. At the same time, the symmetrical structure can return the beam orbit to the original horizontal plane and is better for cancelling nonlinear high-order terms.

To cancel the energy modulation, high-order terms between M and D-M should be carefully corrected. Four families of sextupoles (eight in total) have been added, as shown in Fig. 6. To reduce the effects on nonlinearity

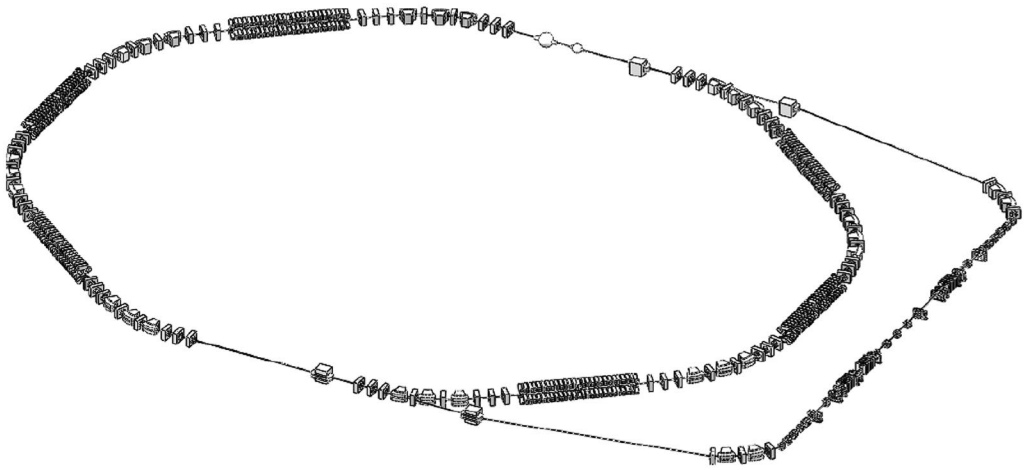

Figure 8. Sketch of damping ring and bypass beam line.

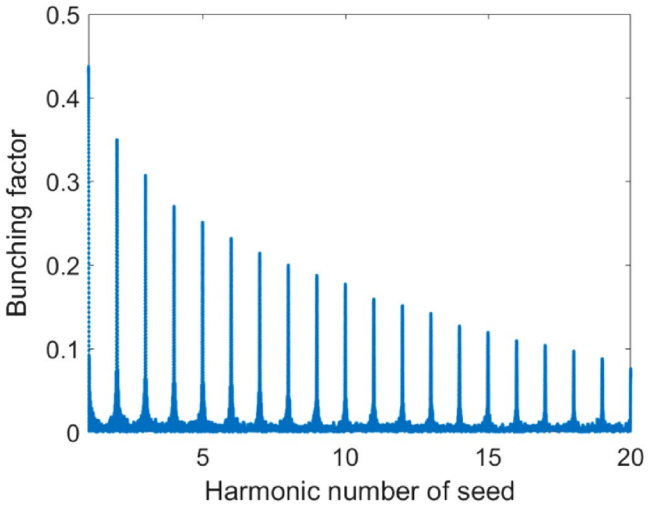

Figure 9. Bunching factor distribution for the ADM.

of the storage ring as well as the linear optics matching, a bypass line has been adopted for the beam manipulation and EUV generation, as shown in Fig. 8. The major part of the bypass beam line consists of three sections: the *core* section between M and D-M is isochronous and with controllable high-order terms; the *dispersion match* section makes the whole beam line achromat in vertical plane; the *Twiss match* section matches the Twiss parameters to the rest part of the beam line.

The storage ring is filled by several bunch trains that can be kicked out to the bypass beam line successively for radiation. This kind of bunch train filling pattern can reduce the technical challenges of the kicker system. The repetition rate of the kicker will be reduced and the pulse width will be increased comparing to the bunch-by-bunch kick out. With this setup, the radiation pulses will be generated in the burst mode. For instance, here we consider an operation mode that 5 bunch trains separated by 14 empty buckets (the last separation gap is 18 buckets) are filled in the ring. Each bunch train holds 38 bunches. In this configuration, the repetition rate of the kicker is 100 kHz, making the kicker field rising time of 20 ns.

Three-dimensional numerical simulations have been performed to show the possible performance of the proposed ring. Main parameters employed in the 3D simulations are given in Table 2. The laser-electron beam interaction in the modulator induces an energy modulation amplitude of about 0.6 times of the initial energy spread (with IBS effect). The bunching factor distribution before entering the radiator (R) is shown in Fig. 9, where one can find that the bunching factor at 19th harmonic (13.55 nm) is about 9%.

Figure 10 shows the residual energy modulation of the electron beam after passing through the whole bypass line. It can be seen that the residual energy modulation is significantly reduced after the optimization of sextupole magnets. The energy spread increases by 0.016% and the vertical emittance increases by 6.89% (RMS) after a single pass. As the horizontal emittance is large and in an irrelevant plane, the emittance growth in horizontal plane is negligible.

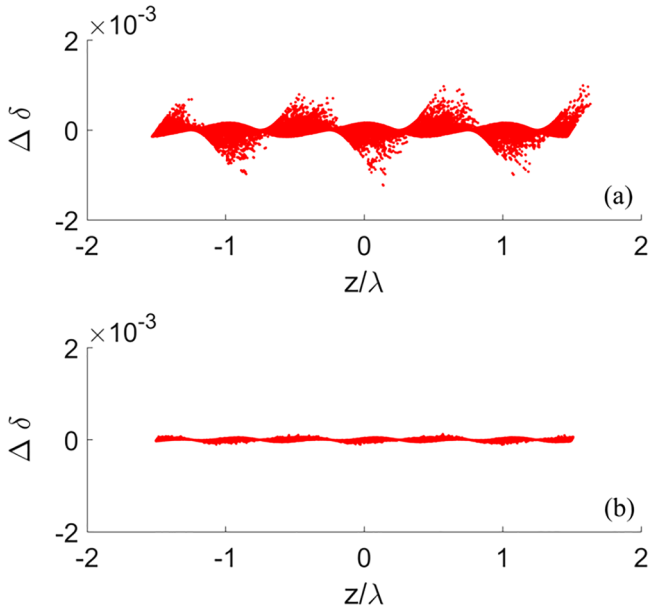

Figure 10. Residual energy modulation before (**a**) and after (**b**) sextupoles optimization.

The electron beam normally circulates in the storage ring. In a short repetition time, the electron beam will be kicked out to the bypass beam line again to interact with the laser and emit EUV radiation. The growth of the energy spread and the vertical emittance per turn is sufficiently small after demodulation, which results an unclear damping process when including quantum exciting effect in the simulation with limited numbers of macro-particles. Therefore, we analyze the repetition rate according to the theoretical formula. The growth of vertical emittance and energy spread will be damped in the storage ring according to the following two formulas[7]:

$$\varepsilon_s(t) = \varepsilon_{s0} e^{-\frac{2t}{\tau_s}}, \tag{3}$$

$$\varepsilon_y(t) = \varepsilon_{y0} e^{-\frac{2t}{\tau_y}}, \tag{4}$$

where ε_s, ε_y are the longitudinal and vertical emittances, ε_{s0}, ε_{y0} are the balanced longitudinal and vertical emittances, τ_s, τ_y are the longitudinal and vertical damping times.

The energy spread growth can be damped down in one turn. As the vertical emittance ε_{y0} is very small which contributes very limited nonlinear effect on the isochronous beam line, the imperfect demodulation is majorly from the longitudinal drift caused by the longitudinal and the horizontal emittances via T_{566}, T_{511}, T_{522} and T_{512} terms. As the energy spread and the horizontal emittance are almost unchanged after demodulation, the growth of the vertical emittance is approximate an absolute value, which is about 0.64 pm·rad. The vertical emittance growth can be damped down in 95 turns. Therefore, the repetition rate of a single bunch is 20 kHz. Assuming the bunch number is 190, the repetition rate of EUV radiation for a single pulse mode is about 3.8 MHz.

The longitudinal profile and the corresponding spectrum of a single EUV radiation pulse simulated by Genesis[25] are shown in Fig. 11. The single pulse energy is about 332 μJ, which is produced by a 3.5 m long undulator with a period length of 2.5 cm. With a repetition rate of 3.8 MHz, the average power is calculated to be about 1.26 kW. There are 2 undulators in the beam line as indicated in Fig. 6 with a canted angle of 19 mrad in vertical plane. The total output average power of the proposed storage ring reaches 2.52 kW.

Discussion

The instabilities should be carefully studied for high current operation of the ring, however, 15.8 mA/bunch current is not an aggressive number. IBS effect has already been estimated in section II. Other issues will not be discussed in this paper in detail. A rough estimation is that multi-bunch instability with an order of magnitude higher current will be damped by an order of magnitude lower damping time comparing to an ordinary storage ring. The vacuum pipe should be carefully designed to avoid wake field energy loss at the small steps to avoid beam pipe been heated.

The radiation power produced per straight section from SWs is about 330 kW which is great but manageable. The radiation divergence from the wiggler is 16.2 mrad and 0.5 mrad in H/V planes respectively. At the end of the wiggler, the diameters of the spot are 139.3 mm (H) and 4.3 mm (V). The size of SW beam pipe can be larger than these values to avoid a major energy dissipate on the SWs beam pipe. The radiation power from SWs can be absorbed by a specially designed high-power absorber in the following arc. Such kind of absorber (256 kW) has been designed for the ILC damping ring[26].

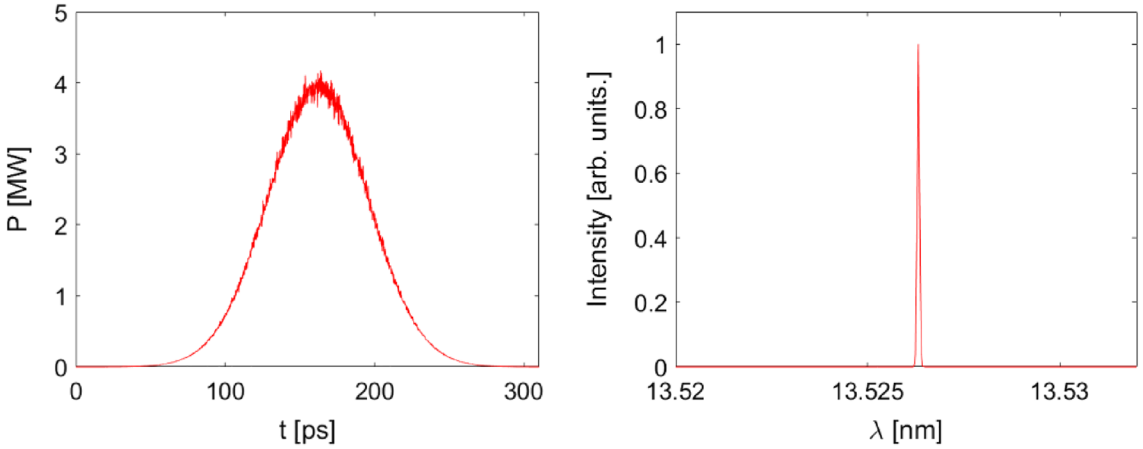

Figure 11. Output radiation pulse and the corresponding single-shot spectrum.

RF system is a tough job for this high current storage ring which should provide 2100 kW RF power to the beam. Due to the low accelerating voltage and high beam loading operation parameters, the normal conducting technology would be adopted. The RF input coupler and the HOM coupler/absorber should be the key components of the main cavities.

2.5 kW EUV radiation can be gotten with 3 A average beam current. The energy transfer efficiency from the electron beam to the EUV radiation is more than 0.1%. The RF power is mainly consumed by SWs. The EUV radiation from each SW is about 19.8 W, it can be collected if it gets value.

The damping ring itself gets outstanding performances with large DA and LMA. We have also tried the case with lower beam energy of 600 MeV, the nature emittance is 0.152 nm·rad which means the normalized beam emittance is only 0.178 μm·rad. This damping ring can be a competitive candidate for the injectors of colliders or free electron lasers.

Received: 21 October 2021; Accepted: 16 February 2022
Published online: 28 February 2022

References

1. Murphy, J. B., White, D. L., MacDowell, A. A. & Wood, O. R. Synchrotron radiation sources and condensers for projection X-ray lithography. *Appl. Opt.* **32**, 6920–6929 (1993).
2. Guiseppe, D. *et al.* Extreme ultraviolet(EUV) sources for lithography based on synchrotron radiation. *Nucl. Instrum. Methods Phys. Res. A* **474**, 259–272 (2001).
3. Lee, J. *et al.* Demonstration of a ring-FEL as an EUV lithography tool. *J. Synchrotron Rad.* **27**, 864–869 (2020).
4. Mitri, S. D. *et al.* Bridging the gap of storage ring light sources and linac-driven free-electron lasers. *Phys. Rev. Accel. Beams* **24**, 060702 (2021).
5. Deng, X. *et al.* Experimental demonstration of the mechanism of steady-state microbunching. *Nature* **590**, 576–579 (2021).
6. Ratner, D. F. & Chao, A. W. Steady-state microbunching in a storage ring for generating coherent radiation. *Phys. Rev. Lett.* **105**, 154801 (2010).
7. Li, C. Feng, C. Jiang, B. &Chao, A. Lattice design for the reversible SSMB. *Proceedings of International Particle Accelerator Conference*. IPAC2019, Melbourne, pp. 1507–1509 (2019).
8. Feng, C. & Zhao, Z. A storage ring based free-electron laser for generating ultra short coherent EUV and X-ray radiation. *Sci. Rep.* **7**, 4724 (2017).
9. Li, C., Feng, C. & Jiang, B. C. Extremely bright coherent synchrotron radiation production in a diffraction-limited storage ring using an angular dispersion-induced microbunching scheme. *Phys. Rev. Accel. Beams* **23**, 110701 (2020).
10. Tang, C. *et al.* An overview of the progress on SSMB. *60thICFA Advanced Beam Dynamics Workshop on Future Light Sources*, Shanghai (2018).
11. Schoerling, D. *et al.* Design and system integration of the superconducting wiggler magnets for the compact linear collider damping rings. *Phys. Rev. Accel. Beams* **15**, 042401 (2012).
12. Ehrlichman, M. *et al.* Intra beam scattering studies at the Cornell electron storage ring test accelerator. *Phys. Rev. Accel. Beams* **16**, 104401 (2013).
13. Crittenden, J. *et al.* Investigation into electron cloud effects in the international linear collider positron damping ring. *Phys. Rev. Accel. Beams* **17**, 031002 (2014).
14. Wiederman, H. *Particle Accelerator Physics II* (Springer, 1993).
15. Khrushchev, S. V. *et al.* 27-Pole 4.2 T wiggler for biomedical imaging and therapy beamline at the Canadian light source. *Nucl. Instrum. Methods Phys. Res. A.* **603**, 7–9 (2009).
16. Patel, Z., Rial, E., George, A. *et al.* Insertion devices at diamond light source: A retrospective plus future developments. *Proceedings of International Particle Accelerator Conference*. IPAC2017, Copenhagen, pp. 1592–1595 (2017).
17. Fedurin, M., Mortazavi, P., Murphy, J. *et al.* Upgrade alternatives for the NSLS superconducting wiggler. *Proceedings of International Particle Accelerator Conference*. PAC07, Albuquerque, pp. 1335–1337 (2007).
18. Malyshev, O., Lucas, J., Collomb, N. *et al.* Mechanical and vacuum design of the wiggler section of the ILC damping rings. *Proceedings of International Particle Accelerator Conference*. IPAC2010, Kyoto, pp. 3563–3565 (2010).
19. Leemann, S. *et al.* Beam dynamics and expected performance of Sweden's new storage-ring light source: MAX IV. *Phys. Rev. Accel. Beams* **12**, 120701 (2009).
20. Travish, G. & Rosenzweig, J. Strong focusing for planar undulators. *AIP Conf. Proc.* **279**, 276 (1992).

21. Pfluger, J. & Nikitina, Yu. M. Undulator schemes with the focusing properties for the VUV-FEL at the TESLA Test Facility. TESLA FEL-Report. 1996-2 (1996).
22. Borland, M. & Berenc, T. User's manual for elegant. Program Version 2020.5 (2020).
23. Goetsch, T., Feikes, J., Ries, M. & Wüstefeld, G. Status of the Robinson wiggler project at the Metrology Light Source. *Proceedings of International Particle Accelerator Conference*. IPAC2015, Richmond, pp. 132–134 (2015).
24. Li, J. Y., Liu, G. F., Xu, W., Li, W. M. & Li, Y. J. A possible approach to reduce the emittance of HLS-II storage ring using a Robinson wiggler. *Chin. Phys. C.* **37**, 107006 (2013).
25. Reiche, S. Genesis 1.3: A fully 3d time-dependent FEL simulation code. *Nucl. Instrum. Meth. A* **429**, 243 (1999).
26. Zolotarev, K. *et al*. SR power distribution along wiggler section of ILC DR. *Proceedings of International Particle Accelerator Conference*. IPAC2010, Kyoto, pp. 3569–3571 (2010).

Acknowledgements

This work is supported by the National Natural Science Foundation of China (No. 11975298, No. 11975300), Shanghai Science and Technology Committee Rising-Star Program (20QA1410100) and Shanghai office for the Promotion of Science and Technology Innovation Center. We thank Ya Zhu and Shengwang Xiang for figure preparation.

Author contributions

All authors conceived the design of the proposed scheme. B.J. majorly contributed on damping wiggler, C.F. majorly contributed on high harmonic generation, C.L., W.W., D.X. majorly contributed on demodulation. Z.B. majorly contributed on ring lattice.

Competing interests

The authors declare no competing interests.

Additional information

Correspondence and requests for materials should be addressed to C.F.

Reprints and permissions information is available at www.nature.com/reprints.

Publisher's note Springer Nature remains neutral with regard to jurisdictional claims in published maps and institutional affiliations.